PCCP

Accepted Manuscript

This is an *Accepted Manuscript*, which has been through the Royal Society of Chemistry peer review process and has been accepted for publication.

Accepted Manuscripts are published online shortly after acceptance, before technical editing, formatting and proof reading. Using this free service, authors can make their results available to the community, in citable form, before we publish the edited article. We will replace this *Accepted Manuscript* with the edited and formatted *Advance Article* as soon as it is available.

You can find more information about *Accepted Manuscripts* in the Information for Authors.

Please note that technical editing may introduce minor changes to the text and/or graphics, which may alter content. The journal's standard Terms & Conditions and the Ethical guidelines still apply. In no event shall the Royal Society of Chemistry be held responsible for any errors or omissions in this *Accepted Manuscript* or any consequences arising from the use of any information it contains.

ROYAL SOCIETY OF CHEMISTRY

www.rsc.org/pccp

Journal Name RSCPublishing

ARTICLE

Improved Photoelectrochemical Water Oxidation Kinetics Using TiO_2 Nanorod Arrays Photoanode Decorated with Graphene Oxide in a Neutral pH Solution

Cite this: DOI: 10.1039/x0xx00000x

Received 00th January 2012,
Accepted 00th January 2012

DOI: 10.1039/x0xx00000x

www.rsc.org/

Sang Youn Chae[a,b], Pitchaimuthu Sudhagar[c], Akira Fujishima[c], Yun Jeong Hwang[a,d*], Oh-Shim Joo[a,d]

We prepared TiO_2 nanorod (NR) arrays on a fluorine-doped tin oxide substrate and decorated with graphene oxide (GO) to study their photoelectrochemical (PEC) water oxidation activities in two different electrolytes. The PEC performances of GO-decorated TiO_2 NR photoanodes were characterized by optical and electrochemical impedance spectroscopy measurements. In 1 M KOH, the photocurrent density of the TiO_2 NR film decreased after deposition of GO, while in the neutral pH electrolyte (phosphate buffered 0.5 M Na_2SO_4), the TiO_2 NR photoanode showed enhanced performance after deposition with the 2 wt% GO solution. This was a consequence of the decrease in charge transfer resistance between the electrode surface and electrolyte. The improvement of photocurrents by GO decoration was obvious near the onset potential of the photocurrents in the neutral pH electrolyte. These opposite contributions of GO on the TiO_2 NR photoanodes suggest that GO can help the water oxidation effectively in a neural electrolyte because depending on pH of the electrolyte, different chemical species interact with the surface of the photoanode in the water oxidation reaction.

Introduction

Solar water splitting has been attractive as a clean and renewable approach for producing hydrogen, wherein the thermodynamically uphill water-splitting reaction ($\Delta E^o = 1.23\ V$) proceeds by utilizing solar energy. Sunlight can be absorbed by semiconductor materials to generate charge carriers that photoelectrochemically oxidize/reduce water. To achieve high solar-to-hydrogen (STH) efficiency, various semiconductor materials have been tested in photoelectrochemical (PEC) applications, and TiO_2 is the most studied material because of its nontoxicity, low cost, and excellent stability for the photo-oxidation of water despite its large bandgap (3.0–3.2 eV). Therefore, various strategies for increasing STH efficiency have been developed using TiO_2 as a model material such as doping[1], morphology control of nanostructured TiO_2[2], surface decoration with cocatalysts[3], and heterojunction formation[4]. For morphology controls, 1-dimensional TiO_2 nanorod (NR) arrays have been demonstrated as a beneficial nanostructure for facile electron transport along the NR[5], and NR arrays can be grown on the conducting substrate easily by one-step hydrothermal synthesis[6]. Most of the previous studies on the photoanodic application of TiO_2, for generating O_2 from water, have been carried out in a strong basic electrolyte, such as aqueous solutions of NaOH or KOH, because TiO_2 is stable and H_2O_2, an intermediate produced during the evolution of O_2, is unstable in basic conditions[7]. However, a strong basic solution has limitations due to its hazards and corrosive property. To increase the absorption efficiency of solar spectrum, wide band gap TiO_2 are coupled with visible light absorbers[8-10]; however, many of them are unstable in strong base or show poor performance[11, 12]. Therefore, studies on the PEC activities of TiO_2 in other electrolytes, including neutral electrolytes, are also important. The main difference between water-oxidation in basic and neutral solutions lies in the chemical species involved in its oxidation. For oxidation of water, OH^- is the dominant species in basic electrolytes, while H_2O molecule is dominant in neutral electrolytes. Therefore, the photocatalytic oxidation of water on TiO_2 surface may have different behaviours in these electrolytes, and suitable surface treatment may be required for developing efficient photocatalysts for neutral electrolytes.

Herein, we study the photo-oxidation activity of TiO_2 NR photoanodes in a neutral pH electrolyte and compare it to that in a basic electrolyte. A hydrothermally prepared TiO_2 NR

array film was decorated with graphene oxide (GO). GO sheets can be chemically tuned for various functions, and their hydrophilic nature makes them more favourable for the aqueous PEC application than graphene sheets, which are hydrophobic and unstable in aqueous reactions[13]. GO and reduced GO have been used in semiconductor photoanodes, such as TiO_2, ZnO, WO_3, $BiVO_4$, and g-C_3N_4[14-17], for improving their charge separation/transport efficiency. It is believed that GO sheets incorporated with semiconductor photocatalysts can serve as an electron sink for separating and storing the photo-excited electrons. Therefore, the charge transfer of from TiO_2 to GO is expected to lead the suppression of electron-hole recombination and charge transfer resistance in the TiO_2 NR photoanode.

Herein, we demonstrate that, in a neutral electrolyte, the photoanodic activities of TiO_2 NRs were improved by the decoration of a small amount of GO; while in a basic electrolyte the presence of GO on TiO_2 NR surfaces decreases the photo-oxidation activities. Electrochemical impedance analysis indicated that the GO decorated onto the TiO_2 NRs improved electron transfer between TiO_2 networks and water oxidation kinetics in the neutral pH solution.

Experimental

Preparation of TiO_2 NR Arrays Photoanode

TiO_2 NRs were directly synthesized on fluorine-doped tin oxide (FTO) coated glass (8Ω, Pilkington) by a hydrothermal method. A 1:30:30 volume ratio of titanium isopropoxide (Aldrich, 97%), distilled water, and concentrated HCl (Aldrich, 37.5%) solution was vigorously stirred prior to the reaction. The mixed solution was transferred into a Teflon-lined autoclave and the FTO substrates were put into the autoclave with most part of the glass being immersed into the solution. TiO_2 NRs were grown at 160°C for 150 min; subsequently, the TiO_2 NR grown FTO substrates were rinsed with deionized water and dried using nitrogen gas prior to annealing at 400°C for 1 h in air.

Preparation of Graphene Oxide

The GO powder was prepared using a modification of Hummer's method[18]. In detail, 1.3 g of graphite powder (natural-325 mesh, purity 99.8% Alfa Aesar) and 2.0 g of $NaNO_3$ were mixed with 70 mL of H_2SO_4 and stirred in an ice bath for 10 min. Subsequently, 9 g of $KMnO_4$ was slowly added and the temperature of the mixture was maintained below 5°C. The above suspension was allowed to stand for 2 h in an ice bath, and was then heated to 40°C in a water bath. Subsequently, the required amount of water was slowly added until the bath temperature reached 98°C; this temperature was maintained for 60 min. Next, water was added to make-up the volume of the suspension to 200 ml and 10 ml of H_2O_2 was added after 5 min. Finally, the product was centrifuged, and washed with water and 5% HCl. The resulting powder was dried at 60°C under ambient atmosphere.

Graphene Oxide Decoration on TiO_2 Nanorod arrays

GO was decorated onto the TiO_2 NR arrays or bare FTO substrate by spin coating. 2 and 5 wt% GO solutions dispersed in absolute ethanol (J. T. Baker, 99.9%) were spin coated at 1000 rpm for 30 s, followed by thermal treatment at 300°C for 5 min to enhance the adhesion of GO onto the substrates.

Photoelectrochemical Measurements

The PEC performance of the GO-decorated TiO_2 NR photoanode was measured by linear sweep voltammetry at a 10 mV/sec scan rate using a potentiostat (Iviumstat) under 1-sun condition (100 mW/cm^2). To simulate sunlight, a solar simulator (ABET, Sun 2000) equipped with a 300 W Xe lamp and 1.5 air mass filter was used, and the incident light was chopped at 0.1 Hz. A potassium phosphate-buffered 0.5 M Na_2SO_4 (pH 7.0) solution and a 1.0 M KOH aqueous solution (pH 13.6) were used as the neutral and basic electrolytes, respectively. 3-electrode measurement was conducted using a Pt counter electrode, an Ag/AgCl reference electrode, and bare or GO-decorated TiO_2 photoanode was used as the working electrode. The applied potentials were converted to potentials versus a reversible hydrogen electrode (RHE) using equation (1)

$$E_{RHE} = E_{Ag/AgCl} + 0.0591 \times pH + E^0_{Ag/AgCl} \quad (1)$$

$$E^0_{Ag/AgCl}\ (3.0M\ NaCl) = 0.209\ V\ at\ 25°C$$

Material Characterization

The prepared GO was characterized by transmittance electron microscopy (TEM) and Raman spectroscopy. The surface morphologies of bare and GO-decorated TiO_2 NRs samples were investigated by scanning electron microscopy (SEM; Hitachi, S-4100). The crystal structure was characterized using an X-ray diffractometer (Shimadzu, XRD-6000), and the transmittances of bare and GO-decorated TiO_2 NR photoanodes were measured using a UV-Vis spectrometer (Varian, Cary 100). Electrochemical Impedance Spectroscopy (EIS) was carried out in the 100 kHz to 0.1 Hz range with applied potential (0.6 V *vs.* RHE) under 1-sun condition; the spectra were fitted using the Z view software (2.8d version).

Result and Discussion

Fig. 1 shows the photograph and SEM images of three distinct TiO_2 NR photoanodes which are bare TiO_2 (TiO_2 NR), TiO_2 decorated with 2 wt% GO solution (2 wt% GO/TiO_2 NR), and TiO_2 decorated with 5 wt% GO solution (5 wt% GO/TiO_2 NR). The synthesis of the GO sheets was confirmed by Raman spectroscopy and a TEM image (Fig. S1 and S2, ESI†), and the rutile crystalline structure of the TiO_2 NRs was confirmed by the X-ray diffraction (XRD) patterns of the three distinct films (Fig. S3, ESI†). The white TiO_2 NR film became slightly darker upon spin-coating with GO solution (Fig. 1a). Visual inspection revealed that the 5 wt% GO/TiO_2 NR film was darker than the 2 wt% GO/TiO_2 NR film; this observation was

consistent with the transmittance spectra (Fig. 2). Top-view SEM images (Fig. 1b–1d) showed that bare TiO_2 NR films had

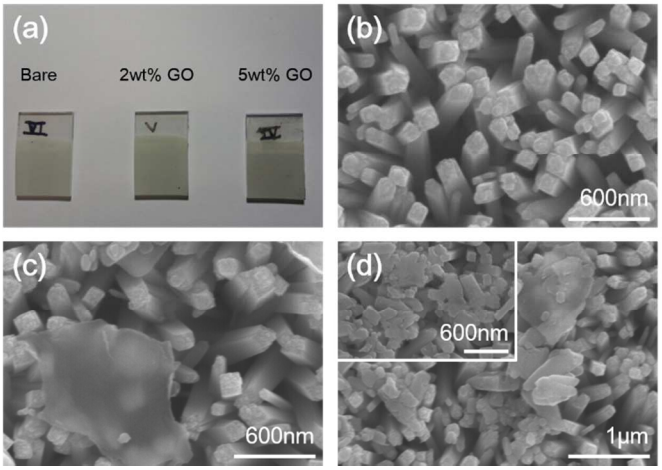

Fig. 1 (a) Photographic images of TiO_2 NR and GO decorated TiO_2 NR films on FTO substrate, and SEM images of each film: (b) bare TiO_2 NR, (c) 2wt% GO/TiO_2 NR, and (d) 5wt% GO/TiO_2 NR. An inset image in (d) is a high magnification image of (d).

rod shaped morphologies (Fig. 1b). The presence of GO fragments or sheets, connecting the NRs, was also observed (Fig. 1c and 1d).

In order to characterize the difference in film color according to the GO deposition condition, the optical properties were analyzed using a UV-vis spectrometer. The UV-vis spectra of the three distinct films on the FTO substrates showed that transmittance in the visible light region decreased after GO decoration (Fig. 2). In the UV region, at wavelengths (λ) shorter than about 380 nm, there was no transmittance for all three samples because of UV light absorption by TiO_2. However, beyond 380 nm, the transmittance increased quickly until λ= ~ 410 nm. The wide band gap of TiO_2 (3.0 eV for rutile TiO_2) only allows efficient light absorption in the UV region. However, transmittance in the visible region (λ=410~800 nm) varied between the three different samples. The transmittance level gradually decreased from bare TiO_2 NR to 2 wt% GO/TiO_2 NR, and 5 wt% GO/TiO_2 NR as the concentration of the GO spin-coating solution increased. This decrease may be associated with the increased scattering induced by the GO fragments. Even though TiO_2 is unable to absorb visible light, bare TiO_2 had less than 50% transmittance because the incident light was scattered by the NR arrays on the FTO glass[19]. GO fragments on the TiO_2 NR film are expected to cause additional scattering, which will further decrease light transmission, resulting in a darker color of GO decorated films, as shown in Fig. 1a.

The PEC performance of each film was studied in two electrolytes with different pH levels, 1 M KOH (Fig. 3a) and 0.5 M Na_2SO_4 phosphate-buffered at pH 7 (Fig. 3b). We observed higher photocurrent densities in the basic electrolyte for all three TiO_2 NR photoanodes regardless of GO deposition

Fig. 2 Transmittance of bare TiO_2 NR, 2wt% GO/TiO_2 NR, and 5wt% GO/TiO_2 NR films on FTO substrates showing lower transmittance in visible range with GO

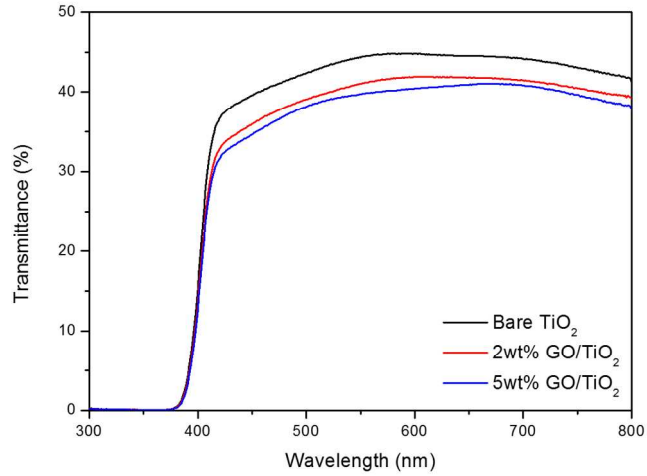

deposition.

condition. The photocurrent density of the bare TiO_2 NR film in 1 M KOH electrolyte was 0.797 mA·cm^{-2} (at 1.23V vs. RHE), which decreased to 0.677 mA·cm^{-2} in the buffered Na_2SO_4 electrolyte (15% decrement). At 1.23V vs. RHE, the photocurrent density of the 2 wt% GO/TiO_2 photoanode decreased from 0.778 mA·cm^{-2} in the KOH electrolyte to 0.767 mA·cm^{-2} in the neutral pH electrolyte, and that of 5 wt% GO/TiO_2 decreased from 0.720 mA·cm^{-2} to 0.703 mA·cm^{-2}. The decrease in both currents was less than 3%. This decrease in photo-oxidation activity in the
neutral electrolyte can be associated to the different water oxidation mechanism (See Scheme S1, ESI†). In a strong base solution, OH^- ions are the main chemical species that are oxidized on the TiO_2 surface, while H_2O molecules participate in a neutral solution. The photo-oxidation mechanism of water on the TiO_2 surface has long been considered to be an electron transfer type reaction[20]. In the initial step, Ti-OH at the surface and OH^- ion in the electrolyte are oxidized by holes to produce Ti-OH• and OH• radicals. In the next step, these radicals combine with each other to form H_2O_2, which is further oxidized by the holes to evolve O_2 molecules. However, Y. Nakato et al. reported that this mechanism is invalid when the pH of the solution is less than ~12 and suggested a Lewis acid-base type reaction mechanism, which involves the oxidation of H_2O molecules[21]. This mechanism is initiated by surface trapped holes and the nucleophilic attack of H_2O molecules. Additional attack of a H_2O molecule forms Ti-O-O-Ti, and then an O_2 molecule is released from the TiO_2 surface[22]. Different reaction pathways, depending on the pH of the electrolyte, can lead to different oxygen evolution rates.

Interestingly, the best performing TiO_2 photoanode was different for each electrolyte. In 1 M KOH, bare TiO_2 NR showed the highest photocurrent in almost every potential region, followed by 2 wt% and 5 wt% GO/TiO_2. Meanwhile, in the buffered Na_2SO_4 neutral electrolyte, the highest photocurrent density was obtained using 2wt% GO/TiO_2 and

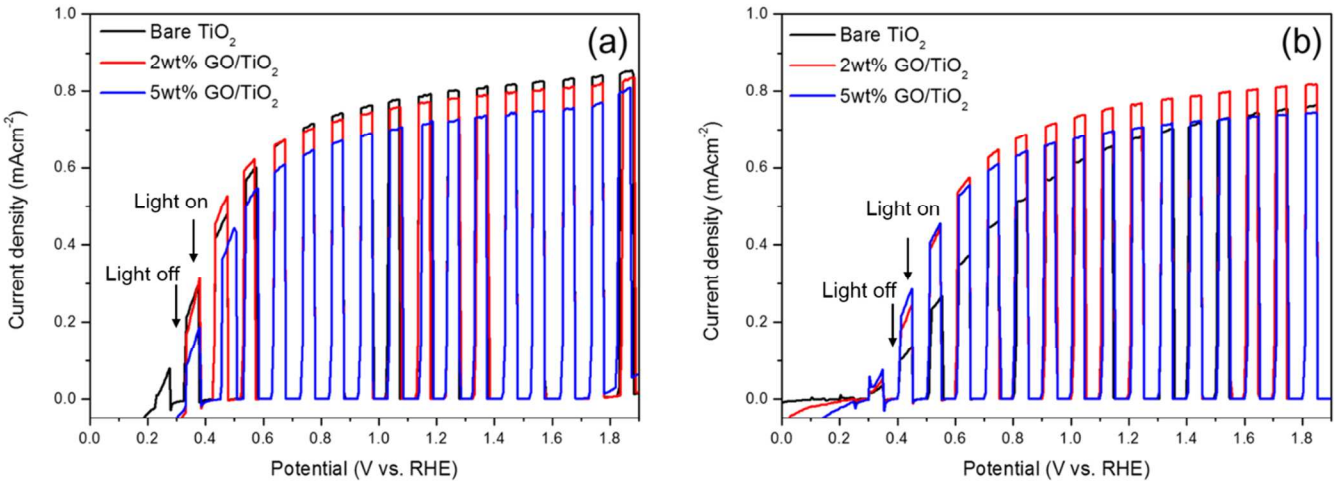

Fig. 3 Linear sweep voltammetries of TiO_2 NR and GO decorated TiO_2 NR photoanodes measured under simulated sunlight in the electrolyte of (a) 1.0M KOH, and (b) 0.5M Na_2SO_4 buffered pH 7.0, respectively.

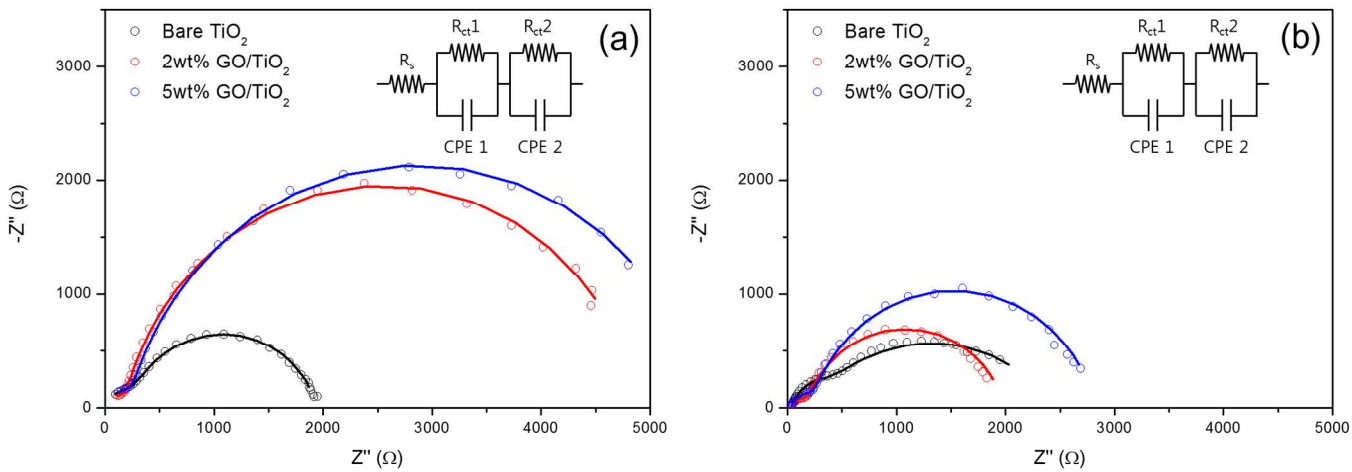

Fig. 4 Nyquist plots of EIS of TiO_2 NR and GO decorated TiO_2 NR photoanodes in the electrolyte of (a) 1.0M KOH, and (b) 0.5M Na_2SO_4 buffered pH 7.0. An equivalent circuit is shown in the inset figure, where R_s is a series resistance of PEC cell, R_{ct1} is a charge transport resistance in internal TiO_2 or GO/TiO_2 film, R_{ct2} is a charge transport resistance between electrolyte and photoanode interface, and CPE is constant phase element. Dots are experimental data and solid lines are fitted one by software.

the bare TiO_2 NRs showed the poorest activity. The most significant increase in photocurrents was observed in the low biased region, around 0.3 ~ 1.23 V vs. RHE, where the fill factor of the current-voltage curve increases after GO deposition. For instance, at 0.7 V vs. RHE, the photocurrent density of the photoanode increased from 0.44 mA·cm^{-2} to 0.63 mA·cm^{-2} after deposition with 2 wt% GO solution, which was close to a 1.5 times improvement. At an even lower bias potential, 0.4 V vs. RHE, the highest photocurrent density was achieved using 5 wt% GO/TiO_2 NR, which showed a photocurrent 2.3 times higher than that of bare TiO_2 NR; 2 wt% GO/TiO_2 showed a 1.9 times improvement in photocurrent. This photocurrent improvement near the onset potential of the photocurrents indicates that GO acts as a co-catalyst and reduces the overpotential for water oxidation.

To understand the different behaviour of the three TiO_2 NR photoanodes, we carried out EIS measurement in each electrolyte (Fig. 4 and Table 1). Inset of Fig. 4 shows the equivalent circuit of the photoanodes for the EIS measurements, wherein R_s, R_{ct1}, and R_{ct2} represent solution resistance, charge transport resistance in internal film (bulk TiO_2 or GO/TiO_2), and charge transfer resistance between photoanode surface and electrolyte, respectively[23]. In the case of 1 M KOH electrolyte (Fig. 4a), 2 wt% GO/ TiO_2 showed a smaller charge transport resistance within the photoanode film (R_{ct2} = 177.33 Ω for 2 wt% GO/TiO_2 and 205.09 Ω for bare TiO_2) and a larger charge transfer resistance between surface and electrolyte (R_{ct2} = 4750 Ω for 2 wt% GO/TiO_2 and 205.09 Ω for bare TiO_2) compared to bare TiO_2 NR. This implies that GO helps electron transport within the TiO_2 NR networks, while it hinders efficient hole transfer from the TiO_2 surface to electrolyte by blocking the catalytic active site for photo-oxidation on the TiO_2 surface. In other words, EIS analysis suggests that the TiO_2 surface is superior to the GO decorated surface for the OH^--mediated electron-transfer type oxidation reaction, which occurs in the KOH electrolyte, as discussed above. In addition, the

deposition of GO sheets onto the TiO_2 NR surface may block incident light by increased scattering, which can decrease the amount of photo-excited carriers in the TiO_2 film. This can cause larger R_{ct2} value after GO deposition, which is consistent with the larger R_{ct2} value observed for the 5 wt% GO/TiO_2 sample.

Table. 1 Fitted values from the EIS analysis.

Sample	Electrolyte	R_{ct} 1 (Ω)	R_{ct} 2 (Ω)	n of CPE 2
Bare TiO_2	1M KOH	205.09	1720	0.817
2wt% GO/TiO_2	1M KOH	177.33	4750	0.876
5wt% GO/TiO_2	1M KOH	224.78	5285	0.863
Bare TiO_2	0.5M Na_2SO_4 [a]	185.64	2245	0.591
2wt% GO/TiO_2	0.5M Na_2SO_4	132.96	1828	0.824
5wt% GO/TiO_2	0.5M Na_2SO_4	204.00	2592	0.853

[a] 0.5 M Na_2SO_4 phosphate-buffered at pH 7.0

On the other hand, in the neutral solution, 2 wt% GO/TiO_2 is expected to improve the charge transfer resistances both within the TiO_2 NR film and across the electrode surface/electrolyte, according to EIS measurement (Table 1). This opposite trend of R_{ct2} with GO deposition suggested that GO can also improve the kinetics of water oxidation on the anode surface because it has better interactions with H_2O molecules in the neutral electrolyte, which boosts the Lewis acid-base type reaction for water photo-oxidation. Another meaningful mention is the change in the n values in CPE2, the constant phase element between the surface and the electrolyte, in the buffered Na_2SO_4 electrolyte, after deposition of GO. Such significant change was not observed in the 1 M KOH electrolyte. The constant phase element is expressed by Equation 2,

$$Z_{CPE} = \frac{1}{C} j\omega^{-n} \quad (2)$$

where C is a real capacitance, j is an imaginary number, and ω is the angular frequency[24]. Here, n is a parameter related to the distortion of the semicircle in resistance-semicircle parallel connection. n = 1 implies that the CPE is an ideal capacitance, and deviation from the ideal capacitance behaviour has a smaller n value, related to microscopic roughness or slow chemical adsorption on the electrode surface[25, 26]. Considering that the NR shape of TiO_2 was maintained even after GO deposition, we can expect that n is more related to chemical adsorption on the electrode surface. The n values of CPE2 increased from 0.591 (bare TiO_2 NR) to 0.824 (2wt% GO/TiO_2 NR), which suggests a stronger interaction between GO and H_2O molecules compared to that between bare TiO_2 and H_2O molecules, consistent with changes in R_{ct2}. The n values of CPE2 were similar for 2 wt% 5 wt% GO/TiO_2 NRs.

Lastly, 5 wt% GO/TiO_2 always had larger charge transport resistances than 2 wt% GO/TiO_2 or bare TiO_2 NR. This is because more GO deposition on the TiO_2 surface blocks more the incident light, as shown in the transmittance of the UV-vis spectra (Fig. 2). This results in a decrease in the light absorption efficiency of TiO_2, a negative effect on the photocatalytic activity. Thus, it was consistent that 5 wt% GO/TiO_2 showed larger R_{ct1} and R_{ct2} values than the other two TiO_2 electrodes, but a similar n value to that of 2 wt% GO/TiO_2.

Conclusions

We demonstrate the influence of the GO decoration onto TiO_2 NR photoanode on the photo-oxidation of water in a basic/neutral electrolyte. GO improves internal charge transportation of the TiO_2 photoanode in both of the electrolytes by helping charge separation in the TiO_2 film, but it can improve water oxidation kinetics only in a neutral electrolyte, which results in a decrease in charge transfer resistance between the anode surface and electrolyte. EIS analysis indicates that the catalytic activity for the oxygen evolution reaction can be improved using the GO/TiO_2 photoanode in the neutral pH electrolyte. Different reaction pathways initiated by OH^- or H_2O, depending on the electrolyte pH conditions, are believed to cause different photocatalytic activities in the GO/TiO_2 NR compared to the bare TiO_2 NR photoanode. Doping or size control of the graphene oxide may allow further improvement in photoelectrochemical water oxidation using TiO_2 NR in a neutral electrolyte.

Acknowledgements

This work was supported by the program of the Korea Institute of Science and Technology (KIST), and by the Korea Center for Artificial Photosynthesis (KCAP) located in Sogang University funded by the Minister of Science, ICT, and Future Planning (MSIP) through the National Research Foundation of Korea (No. 2014M1A2A2070004)

Notes and references

[a] *Clean Energy Research Center, Korea Institute of Science and Technology (KIST), 39-1 Hawolgock Dong, Seoul 136-791, Republic of Korea. Fax: +82 2 958 5809; Tel: +82 2 958 5227; E-mail: yjhwang@kist.re.kr*
[b] *Department of Chemistry, College of Science, Korea University, Anam Dong, Seoul 136-713, Republic of Korea.*
[c] *Photocatalysis International Research Center(PIRC), Research Institute for Science and Technology, Tokyo University of Science, 2641 Yamazaki, Noda, Chiba 278-8510, Japan*
[d] *Korea University of Science and Technology, 176 Gajung-dong, 217 Gajungro Yuseong-gu, Daejeon 305-350, Republic of Korea*

† Electronic Supplementary Information (ESI) available: [Raman spectrum and TEM images of the prepared graphene oxide, XRD patterns of the three TiO_2 NR photoanodes, and schematic diagram of the proposed mechanism for water oxidation on the TiO_2 surface]. See DOI: 10.1039 / b000000x/

1. I. S. Cho, C. H. Lee, Y. Z. Feng, M. Logar, P. M. Rao, L. L. Cai, D. R. Kim, R. Sinclair and X. L. Zheng, *Nature communications*, 2013, 4.
2. G. Liu, C. H. Sun, H. G. Yang, S. C. Smith, L. Z. Wang, G. Q. Lu and H. M. Cheng, *Chem Commun*, 2010, 46, 755-757.
3. X. J. Lv, S. X. Zhou, C. Zhang, H. X. Chang, Y. Chen and W. F. Fu, *J Mater Chem*, 2012, 22, 18542-18549.
4. Y. J. Hwang, A. Boukai and P. D. Yang, *Nano letters*, 2009, 9, 410-415.

5. Y. X. Gan, B. J. Gan and L. S. Su, *Mater Sci Eng B-Adv*, 2011, 176, 1197-1206.
6. B. Liu and E. S. Aydil, *J Am Chem Soc*, 2009, 131, 3985-3990.
7. M. Tomkiewicz and H. Fay, *Appl Phys*, 1979, 18, 1-28.
8. J. A. Seabold, K. Shankar, R. H. T. Wilke, M. Paulose, O. K. Varghese, C. A. Grimes and K. S. Choi, *Chem Mater*, 2008, 20, 5266-5273.
9. A. Paracchino, V. Laporte, K. Sivula, M. Gratzel and E. Thimsen, *Nature Materials*, 2011, 10, 456-461.
10. F. L. Su, J. W. Lu, Y. Tian, X. B. Ma and J. L. Gong, *Phys Chem Chem Phys*, 2013, 15, 12026-12032.
11. K. Maeda and K. Domen, *J Phys Chem C*, 2007, 111, 7851-7861.
12. A. Kudo and Y. Miseki, *Chem Soc Rev*, 2009, 38, 253-278.
13. T. F. Yeh, J. Cihlar, C. Y. Chang, C. Cheng and H. S. Teng, *Mater Today*, 2013, 16, 78-84.
14. Y. H. Ng, A. Iwase, A. Kudo and R. Amal, *J Phys Chem Lett*, 2010, 1, 2607-2612.
15. P. Wang, Y. M. Zhai, D. J. Wang and S. J. Dong, *Nanoscale*, 2011, 3, 1640-1645.
16. X. J. Liu, L. K. Pan, Q. F. Zhao, T. Lv, G. Zhu, T. Q. Chen, T. Lu, Z. Sun and C. Q. Sun, *Chem Eng J*, 2012, 183, 238-243.
17. J. Q. Tian, Q. Liu, A. M. Asiri, K. A. Alamry and X. P. Sun, *Chemsuschem*, 2014, 7, 2125-2130.
18. W. S. Hummers and R. E. Offeman, *J Am Chem Soc*, 1958, 80, 1339-1339.
19. W. Q. Peng, M. Yanagida, L. Y. Han and S. Ahmed, *Nanotechnology*, 2011, 22.
20. M. R. Hoffmann, S. T. Martin, W. Y. Choi and D. W. Bahnemann, *Chemical Reviews*, 1995, 95, 69-96.
21. R. Nakamura and Y. Nakato, *J Am Chem Soc*, 2004, 126, 1290-1298.
22. R. Nakamura, T. Okamura, N. Ohashi, A. Imanishi and Y. Nakato, *J Am Chem Soc*, 2005, 127, 12975-12983.
23. J. Y. Kim, G. Magesh, D. H. Youn, J. W. Jang, J. Kubota, K. Domen and J. S. Lee, *Sci Rep-Uk*, 2013, 3.
24. G. J. Brug, A. L. G. Vandeneeden, M. Sluytersrehbach and J. H. Sluyters, *J Electroanal Chem*, 1984, 176, 275-295.
25. Z. Kerner and T. Pajkossy, *Electrochim Acta*, 2000, 46, 207-211.
26. T. Pajkossy and D. M. Kolb, *Electrochim Acta*, 2001, 46, 3063-3071.